

## Supplemental Material

### Detailed Methods Online Data Supplement

**Mouse heart valve collection.** The elastin mutant mice were created using a typical gene targeting approach. Specifically, wild type (*Eln*<sup>+/+</sup>) and elastin insufficient (*Eln*<sup>+/-</sup>) mice were derived on a mixed genetic background and a pure C57BL6 line was developed.<sup>1</sup> Mice were maintained by littermate crossings and studied on the following postnatal days (stages): 5 (neonatal), 30 (juvenile), 120 (adult), and 480 (aged adult). Null (*Eln*<sup>-/-</sup>) mice were studied at the neonatal stage only. Mice were genotyped as previously described.<sup>2</sup> The Institutional Animal Care and Use Committee at Cincinnati Children's Hospital Medical Center approved all protocols used.

**Histochemistry and immunohistochemistry.** Valve tissue from 5 mice per genotype per stage was processed and analyzed as previously described.<sup>3</sup> Movat's modified pentachrome stain was used to examine valve ECM and VIC organization. Hart's stain was used to assess elastin expression. Alizarin Red and von Kossa stains were used to evaluate the presence of calcification. TGF- $\beta$  signaling was assessed using rabbit polyclonal antibodies directed against phospho-Smad-2 (pSmad2, Cell Signaling, 1:100) and antigen retrieval. Cell proliferation and apoptosis were assessed using rabbit polyclonal antibodies directed against phospho-Histone H3 (HisH3, Upstate, 1:100) and cleaved caspase-3 (Cas3, Cell Signaling, 1:200), respectively. The immunoreactivity index (positive nuclei/total nuclei) was calculated for TGF- $\beta$  signaling (pSmad2), proliferation (HisH3), and apoptosis (Cas3). Mouse monoclonal antibodies directed against alpha smooth muscle actin (SMA, Sigma, 1:500) and nonmuscle myosin heavy chain (SMemb, Abcam, 1:500) were used to evaluate VIC phenotype.<sup>4</sup> A universal streptavidin/biotin and diaminobenzidine detection system (Pierce) was used for colorimetric detection. Comprehensive aortic valve morphometrics were obtained using ImageJ software (NIH) as previously described.<sup>3,5</sup>

**Biomechanical testing.** To document disease progression in the aorta resulting from elastin haploinsufficiency, mechanical properties were determined in *Eln*<sup>+/-</sup> mice at juvenile and adult stages (6-7 mice were studied per genotype per stage). Segments of aortas (average length 10 $\pm$ 3 mm) were placed into custom grips attached to an electromechanical testing system (Model 100R, Test Resources Inc.). Each sample was stretched longitudinally to a tare load of ~0.08N and then at a constant strain rate of 1%/min to failure. Force and elongation were recorded at a sampling frequency of 30Hz. Tensile stiffness was calculated as the slope in the linear region of the force-elongation curve using MATLAB (MathWorks, Inc.).<sup>6</sup>

**Electron microscopy.** Ultrastructural analysis of mouse valve tissue (n=3 per genotype) was performed using an Hitachi 7600 (Hitachi Technologies) as previously described.<sup>3</sup> For visualization of collagens and elastins, sections were stained with aqueous solutions of 5% tannic acid and 1% uranyl acetate, then counterstained with lead citrate.<sup>7</sup>

**Gene expression profile.** For gene expression comparison, four experimental groups were created as follows: aortic valve *Eln*<sup>+/+</sup>, aortic valve *Eln*<sup>+/-</sup>, ascending aorta *Eln*<sup>+/+</sup>, and ascending aorta *Eln*<sup>+/-</sup>. Aortic valve (including the valve annulus and root) and ascending aorta was dissected from a juvenile mouse and used in one experiment, ie. there was no tissue pooling. Four biological replicates were performed. The juvenile stage was chosen to be after elastin was expressed in the valve and before the onset of disease, which would cause hemodynamic perturbation and secondary ECM remodeling. Since the groups compared gene expression in tissue from heterozygous mutants versus wild type, a threshold of 1.5 fold up or down was considered significant. Differentially expressed genes were selected based on known functional roles in valve and artery development. Data were analyzed using Ingenuity Pathway Analysis (Ingenuity® Systems, www.ingenuity.com). Microarray data are accessible in the Gene

Expression Omnibus ([www.ncbi.nlm.nih.gov/geo/](http://www.ncbi.nlm.nih.gov/geo/)) using the accession number GSE16012.

**Gene Profile Analysis.** RNA was isolated using Trizol (Invitrogen), and the quality of the RNA was checked using the Agilent Bioanalyzer 2100 (Hewlett Packard) and the RNA 6000 Pico Assay. Subsequently, RNA was amplified using WT-Ovation Pico RNA Amplification System Version 1.0 (Nugen), and labeled using FL-Ovation cDNA Biotin Module V2 (Nugen). The target was hybridized to a GeneChip Mouse Genome 430 2.0 Array (Affymetrix) using standard protocols. Arrays were washed and stained using the Fluidics Station 450 and scanned using the GeneChip scanner 3000 (Affymetrix). After filtering for intensity values >100, 19,002 probe sets (42%) were identified as expressed and used for further analysis. The scanned gene expression data were exported as “.CEL” files, which were loaded into GeneSpring Gx 7.3 software (Agilent technologies) and subjected to RMA (Robust Multichip Average) analysis for quantile normalization. Each gene was normalized to the median value of that gene. Canonical pathways analysis identified the pathways from the Ingenuity Pathways Analysis library of canonical pathways that were most significant to the data set. Genes from the data set that met the cutoff and were associated with a canonical pathway in the Ingenuity Pathways Knowledge Base were considered for the analysis. Fisher’s exact test was used to calculate a *p*-value determining the probability that the association between the genes in the dataset and the canonical pathway is explained by chance alone.

**Quantitative real time RT-PCR.** To confirm microarray gene expression analysis, quantitative real time RT-PCR was performed in biologic genes of interest as previously described.<sup>8</sup> Primer sequences are shown in Supplemental Table III.

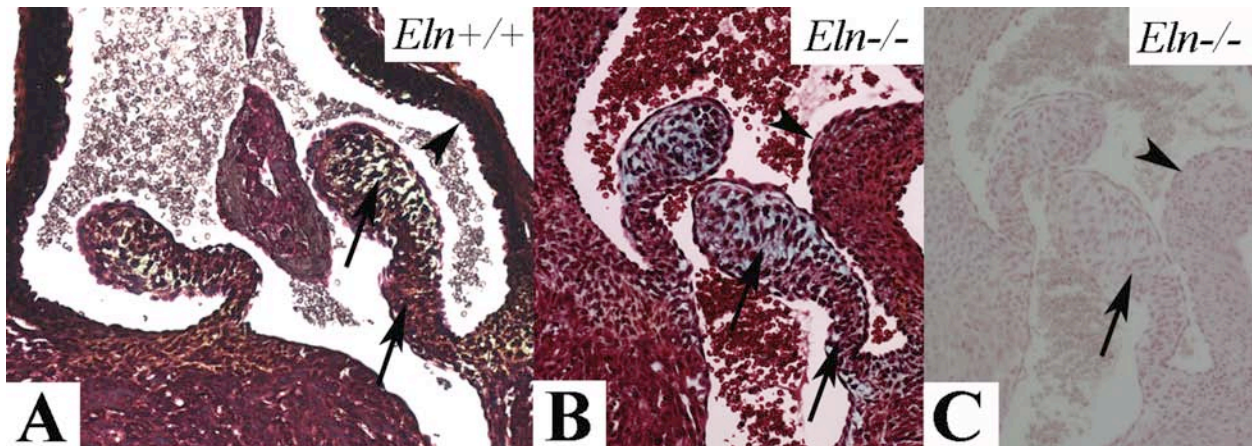
**Echocardiography.** To assess the natural history of elastin haploinsufficiency, in vivo valve structure and function was evaluated using a VisualSonics Vevo 770 transthoracic echocardiography imaging system (VisualSonics, Inc.) in juvenile, adult and aged adult mice, as previously described.<sup>5</sup> At least 10 mice per genotype per stage were studied. The presence of aortic valve disease (stenosis or regurgitation) was assessed by Doppler interrogation. Aortic regurgitation was defined as valve incompetence with reversal of flow in diastole and was determined to be moderate if flow reversal was holodiastolic with a peak velocity  $\geq$  2m/sec. Aortic stenosis was defined as a peak velocity  $\geq$  2m/sec. Mice with left ventricular systolic dysfunction were excluded.<sup>5</sup>

**Statistical analysis.** Findings are reported as mean with either standard deviation or standard error of the mean as appropriate. Student’s t-test was used to compare groups. Univariate or multivariate two-way ANOVA was used to determine the effects of age and genotype on morphometrics by histochemistry, aortic tensile stiffness by mechanical testing, and disease incidence by echocardiography. A *p* value < 0.05 was considered significant.

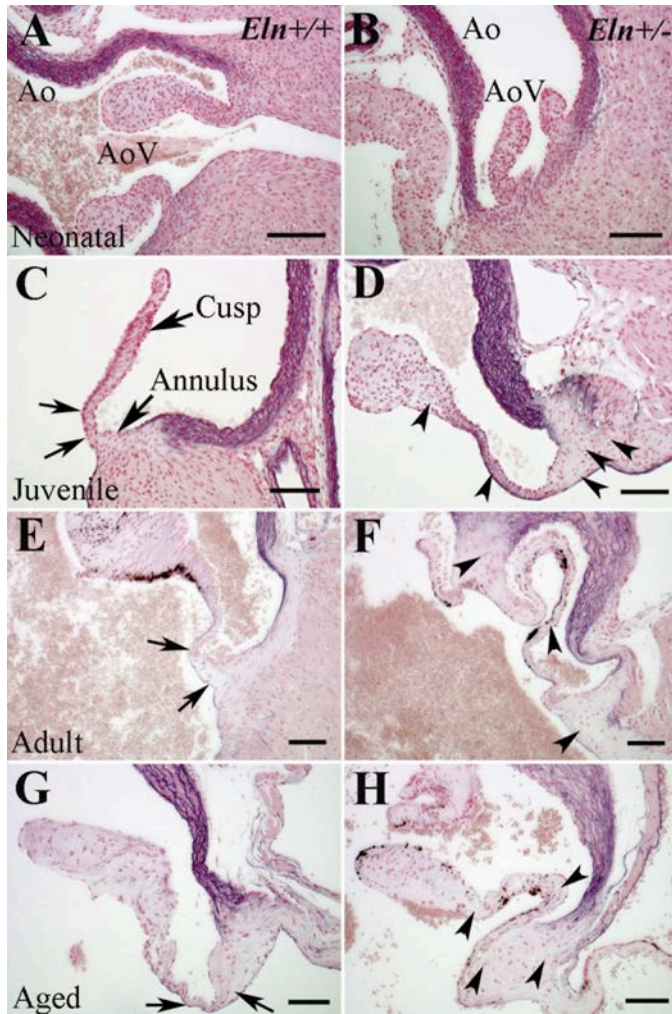
## References

1. Li DY, Brooke B, Davis EC, Mecham RP, Sorensen LK, Boak BB, Eichwald E, Keating MT. Elastin is an essential determinant of arterial morphogenesis. *Nature*. 1998;393:276-280.
2. Faury G, Pezet M, Knutsen RH, Boyle WA, Heximer SP, McLean SE, Minkes RK, Blumer KJ, Kovacs A, Kelly DP, Li DY, Starcher B, Mecham RP. Developmental adaptation of the mouse cardiovascular system to elastin haploinsufficiency. *J Clin Invest*. 2003;112:1419-1428.
3. Hinton RB, Lincoln J, Deutsch GH, Osinska H, Manning PB, Benson DW, Yutzey KE. Extracellular matrix remodeling and organization in developing and diseased aortic valves. *Circ Res*. 2006;98:1431-1438.
4. Aikawa E, Whittaker P, Farber M, Mendelson K, Padera RF, Aikawa M, Schoen FJ. Human semilunar cardiac valve remodeling by activated cells from fetus to adult: implications for postnatal adaptation, pathology, and tissue engineering. *Circulation*. 2006;113:1344-1352.

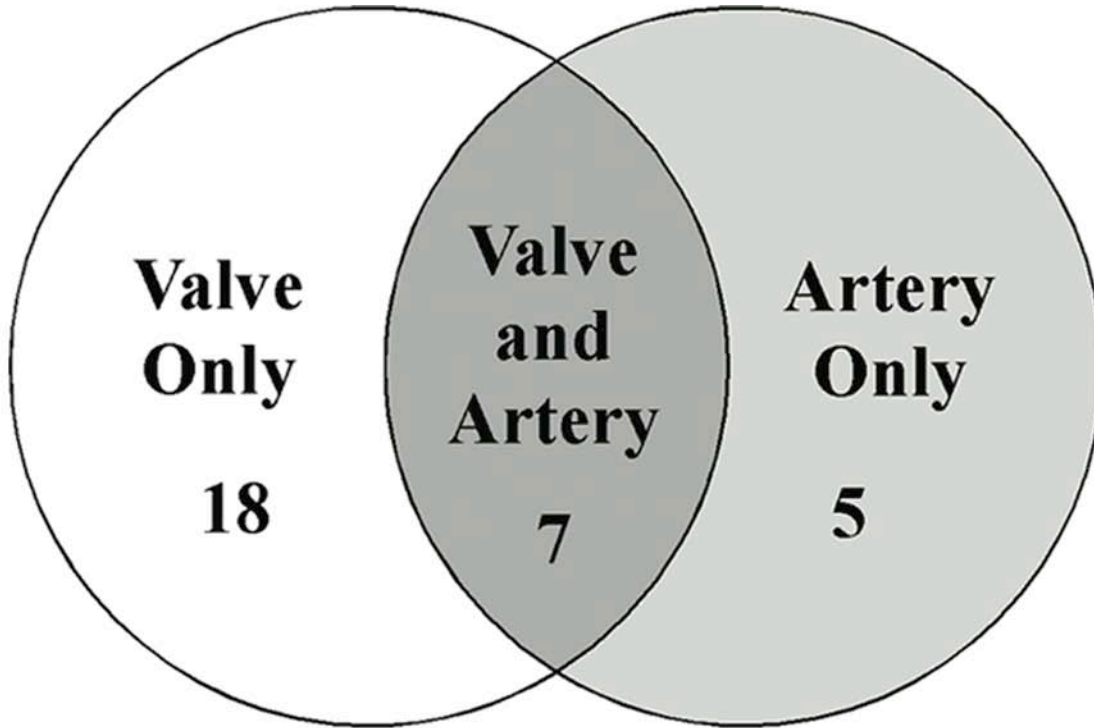
5. Hinton RB, Alfieri CM, Witt SA, Glascock BJ, Khoury PR, Benson DW, Yutzey KE. Mouse heart valve structure and function: echocardiographic and morphometric analyses from the fetus through the aged adult. *Am J Physiol Heart Circ Physiol.* 2008;294:H2480-2488.
6. Vouyouka AG, Pfeiffer BJ, Liem TK, Taylor TA, Mudaliar J, Phillips CL. The role of type I collagen in aortic wall strength with a homotrimeric. *J Vasc Surg.* 2001;33:1263-1270.
7. Hayat M. *Principles and Techniques of Electron Microscopy*: Cambridge University Press; 2000.
8. Zhao B, Etter L, Hinton RB, Benson DW. BMP and FGF regulatory pathways in semilunar valve precursor cells. *Dev Dyn.* 2007;236:971-980.



**Supplemental Figure I. Aortic valve anatomy in neonatal *Eln*<sup>-/-</sup> mice by histochemistry.** In neonatal *Eln*<sup>+/+</sup> mice, there is bilaminar ECM organization of the aortic valve with elastin present in the ventricularis layer (arrows, A, pentachrome stain) and there are organized lamellae in the aorta. In *Eln*<sup>-/-</sup> mice, there appears to be normal bilaminar ECM organization (arrows, B, pentachrome stain) in the aortic valve, and aortic valve morphometrics are normal (data not shown). However, there is no evidence of elastin in the aortic valve ventricularis (arrow, C) or aorta (arrowhead, C) as evidenced by Hart's stain. The aorta is significantly thicker in *Eln*<sup>-/-</sup> mice (arrowheads, B vs. A), consistent with previous studies demonstrating compensatory increased vascular smooth muscle.



**Supplemental Figure II. Elastin expression over time in *Eln*<sup>+/-</sup> aortic valves by histochemistry.** Aortic valve (AoV) cusps in *Eln*<sup>+/+</sup> (A,C,E,G) and *Eln*<sup>+/-</sup> (B,D,F,H) mice at neonatal (A,B), juvenile (C,D), adult (E,F), and aged adult (G,H) stages. Elastin is strongly expressed in the aorta (Ao) at all stages and modestly expressed in the proximal ventricular aspect of the valve cusp at juvenile, adult and aged adult stages (arrows). The *Eln*<sup>+/-</sup> mice demonstrate elastic fiber fragmentation and dispersion in the cusp, and infiltration of elastin fragments into the valve annulus (arrowheads). Scale bar 100 $\mu$ m.



Fibrogenesis pathway subanalysis of differentially expressed genes in <i>Eln</i> <sup>+/-</sup> mice						
Aortic Valve only		Aortic Valve and Aorta			Aorta only	
Gene	Fold Change	Gene	Fold Change Valve	Fold Change Aorta	Gene	Fold Change
<i>Myh-6</i>	+ 2.5	<i>Vegf-b</i>	+ 1.9	- 1.5	<i>Figf</i>	+ 2.2
<i>Agt-r1</i>	+1.9	<i>Myl-3</i>	+ 1.9	- 1.7	<i>Tnfrsf-1b</i>	+ 1.8
<i>Myl-1</i>	+ 1.8	<i>Myl-7</i>	+ 1.7	+ 1.6	<i>Tnfrsf-11b</i>	+ 1.6
<i>Ccr-5</i>	+ 1.6	<i>Fgf-1</i>	+ 1.6	+ 1.6	<i>Ednrb</i>	+ 1.6
<i>Ednra</i>	+ 1.6	<i>Myl-4</i>	+ 1.4	+ 1.5	<i>Vcam-1</i>	+ 1.6
<i>Ccl-21</i>	+ 1.5	<i>Igf-1r</i>	- 1.5	- 1.5		
<i>Kdr</i>	+ 1.5	<i>Pdgf-ra</i>	- 1.6	+ 1.5		
<i>Myl-2</i>	+ 1.5					
<i>Fgf-2</i>	- 1.5					
<i>Ifna-r1</i>	- 1.5					
<i>Ly-96</i>	- 1.5					
<i>Bcl-2</i>	- 1.7					
<i>Cyp-2e1</i>	- 1.7					
<i>Lepr</i>	- 1.7					
<i>Smad-3</i>	- 1.7					
<i>Tgfb-r1</i>	- 1.7					
<i>Myh-11</i>	- 1.9					
<i>Acta-2</i>	- 2.7					

**Supplemental Figure III. Differential gene expression signaling pathway subanalysis.** Within the Fibrogenesis signaling pathway, 30 genes are differentially expressed of which 18 are valve only, 5 are aorta only and 7 are both valve and aorta (overlap). *Tgfb-r1* and *Smad3* are decreased in valve only tissue and not aorta tissue, consistent with spatially restricted TGF- $\beta$  mediated fibrogenesis abnormalities.

**Supplemental Table I. Microarray gene expression validation in *Eln*<sup>+/-</sup> vs. *Eln*<sup>+/+</sup> aortic valve tissue**

Gene	Microarray	qRT-PCR
<i>Tgfb-r1</i>	- 1.7	- 1.4
<i>Myh-11</i>	- 1.7	- 1.7
<i>Smad-3</i>	- 1.7	- 1.2
<i>Hapln-1</i>	- 1.7	- 1.7
<i>Mmp-15</i>	+ 2.4	+ 1.3

**Supplemental Table II. Signaling pathways identified by differentially expressed genes in *Eln*<sup>+/-</sup> mice**

		Aortic Valve	
Signaling Pathway	<i>p</i> -value	Altered genes	
Fibrogenesis	0.00001	<i>Myh-11, Acta-2, Fgf-1, Fgf-2, Pdgf-ra, Agtr-1, Vegf-b, Myh-6, Tgfb-r1, Smad-3, Myl-1, Myl-2, Myl-3, Myl-4, Myl-7, Ccr-5, Igf-1r, Ifna-r1, Cyp-2e1, Ccl-21, Edn-ra, Lepr, Ly-96, Bcl-2, Kdr</i>	
Integrin	0.00004	<i>Itga-8, Actn-1, Rock-1, Parvb, Akt-3, Acta-2, Itga-9, Actg-2, Arhgap-26, Myl-7, Arhgap-5, Tm, Braf, Mylk, Bcar-3, Actn-2, Mlck, Itgb-3, Myl-2, Pik-3c2a, Src, Ppp-1r12a, itga-3, Itga-5, Itga-6, Tspan-5, Atn-4, Acta-1, Arf-4, Tspan-2, Zyx</i>	
Actin Cytoskeleton	0.0002	<i>Tiam-2, Myh-11, Pip-4k2b, Actn-1, Rock-1, Iqgap-1, Acta-2, Fgf-2, Myl-3, Actg-2, Fgf-1, Myl-7, Tm, Mylk, Actn-2, Fgf-12, Mlck, Myl-1, Myl-2, Myl-4, Pik-3c2a, Pdgfd, Diaph-1, Ppp-1r12a, Itga-3, Myh-6, Vav-3, Pdgf-c, Pip-5k1a, Actn-4, Acta-1</i>	
VEGF	0.003	<i>Actn-1, Actn-2, Actn-4, Acta-1, Acta-2, Actg-2, Rock-1, Akt-3, Pik-3c2a, Vegf-b, Ywhae, Eif-2s3, Bcl-2, Kdr</i>	
		Aorta	
Signaling Pathway	<i>p</i> -value	Altered genes	
Fibrogenesis	0.002	<i>Fgf-1, Vegf-b, Ednrb, Myl-7, Vcam-1, Igf-1r, Myl-3, Myl-4, Pdgfra, Figf, Tnfrsf-1b, Tnfrsf-11b</i>	
FGF	0.01	<i>Prkca, Fgf-1, Crk, Mapk-14, Map-2k6, Pik-3c2a, Creb-3</i>	
VEGF	0.01	<i>Prkca, Vegf-b, Eif-2s3, Rock-1, Eif-2s2, Pik-3c2a, Figf</i>	
Notch	0.04	<i>Maml-2, Dtx-4, Notch-3, Hey-1</i>	

**Supplemental Table III. Primers for qRT-PCR**

Gene	Annealing Temperature ( <sup>0</sup> C)	Product Size (bp)	Primer Sequences
<i>Myh-11</i>	57	214	5'-GAAATGGACGCTCGGGACT-3' 5'-CCCTTTGTGCAGGGCTGT-3'
<i>Hapln-1</i>	54	224	5'-CGCTTTGTAGGTTTCCCAGA-3' 5'-TGGCCTTTATGAAAACGACTC-3'
<i>Mmp-15</i>	55	211	5'-GACAGTGAACGTGGTGATGG-3' 5'-CATCTGGGATCCACACGTC-3'
<i>Tgfb-r1</i>	60	172	5'-CACAACTCAGCCAACAGGAA-3' 5'-GGGAAGCTTTCAGTTGACCA-3'
<i>Smad-3</i>	60	187	5'-ACAAGGTCCTCACCCAGATG-3' 5'-AGAAACAGGCTGGTGCCTTA-3'

**Supplemental Table IV. Echocardiographic evaluation of aortic dimensions in *Eln*<sup>+/-</sup> mice**

	Juvenile		Adult		Aged Adult	
	<i>Eln</i> <sup>+/+</sup>	<i>Eln</i> <sup>+/-</sup>	<i>Eln</i> <sup>+/+</sup>	<i>Eln</i> <sup>+/-</sup>	<i>Eln</i> <sup>+/+</sup>	<i>Eln</i> <sup>+/-</sup>
Heart Rate (beats/min)	467±94	447±45	465±60	429±38	428±70	434±55
Animal Weight (grams)	11.2±1.0	10.6±2.3	17.3±1.4	21.7±3.7	33.0±6.0	35.5±3.0
Aortic Valve Annulus (mm)	1.03±0.06	0.96±0.14	1.21±0.07	1.20±0.10	1.16±0.09	1.29±0.05*
Aortic Root (mm)	1.05±0.07	1.02±0.17	1.23±0.07	1.33±0.08	1.15±0.10	1.38±0.18*
Ascending Aorta (mm)	1.18±0.09	1.04±0.20	1.39±0.10	1.34±0.06	1.36±0.10	1.43±0.10

\* $p < 0.05$  *Eln*<sup>+/+</sup> vs. *Eln*<sup>+/-</sup>